Organic & Biomolecular Chemistry

Accepted Manuscript

ROYAL SOCIETY OF CHEMISTRY

www.rsc.org/obc

Journal Name

RSCPublishing

ARTICLE

Design and Synthesis of a Multivalent Fluorescent Folate–Calix[4]arene Conjugate: Cancer Cell Penetration and Intracellular Localization

Cite this: DOI: 10.1039/xoxxoooooox

Received ooth January 2012,
Accepted ooth January 2012

DOI: 10.1039/xoxxoooooox

www.rsc.org/

Grazia Maria Letizia Consoli,[a]* Giuseppe Granata,[a] Giorgia Fragassi,[b] Mauro Grossi,[b] Michele Sallese,[b]* Corrada Geraci[a]

A novel fluorescently labeled folate conjugate in which four folic acid units are covalently conjugated with a 7-nitro-benzofurazan fluorophore by means of a calix[4]arene platform was synthesized by using a Cu-catalyzed azide-alkyne cycloaddition reaction (Click Chemistry). The synthesized construct (FA-C4-NBD) was characterized by mass spectrometry, NMR and fluorescence spectroscopy. Confocal fluorescence microscopy experiments were carried out to evaluate the cell penetration ability of FA-C4-NBD on normal and cancer cells. The cellular uptake of FA-C4-NBD proceeds via folate receptor-mediated endocytosis. FA-C4-NBD is internalized into HeLa cancer cells which express high levels of folate receptor, whereas the uptake into fibroblast NIH3T3 cells which have very low expression levels of folate receptor is negligible. The involvement of the folate receptor was corroborated by competition tests with free folic acid. Co-localization analysis with different organelle markers indicated that FA-C4-NBD is not eliminated by recycling towards the outside of the cell, but accumulates intracellularly in the endo-lysosomal system.

Introduction

Advanced technologies have led to the discovery of a variety of drugs for the treatment and imaging of cancer, but many problems including toxic side effects have yet to be resolved. Targeted drug delivery which is the delivery of a chemotherapeutic or imaging agent only in its site of action is a strategy to target cancer cells while sparing normal cells, thus minimizing toxic side effects and maximizing therapeutic and diagnostic index.

In the research of more effective targeted drug delivery systems, the folate receptor (FR) overexpressed on cancer cells and activate macrophages has emerged as an efficient target.[1,2] The property of folic acid (FA) ligand to maintain high FR binding affinity ($K_D \sim 10^{10}$ M) and cell penetration ability also after conjugation to bioactive molecules and molecular scaffolds, has stimulated the production of a variety of monovalent and multivalent folate conjugates.[3-7] Some folate conjugates have entered clinical trials for the treatment[8] and diagnosis[9] of human cancers, and are under evaluation for therapy[10] and diagnosis[11] of severe inflammatory diseases. Interestingly, fluorescent folate–dye conjugates besides to selectively identify malignant cells, have been also proposed to localize hidden tumor tissues during surgery, detect circulating tumor cells in the peripheral vasculature, and evaluate real time the rate and extent of folate conjugate penetration.[12]

The multivalency effect, for which multiple FA ligands exposed on a molecular scaffold bind multiple FRs organized in cluster on the cancer cell surface, is a valid approach to increase FA to FR binding avidity.[13-15]

Calix[n]arene macrocycles by virtue of synthetic versatility, well-defined structure, low toxicity and immunogenicity are proving valid platforms for the obtainment of multivalent constructs appealing in biomedical and pharmaceutical field.[16] In this regard, we also reported multivalent calixarene derivatives able to elicit a higher biological activity[17-19] and receptor binding avidity[20] than monovalent analogues. Calixarene-based nanoaggregates have been proposed as gene and drug delivery systems,[21] but at the best of our knowledge no study has described a receptor-mediated cellular uptake mechanism for cell-penetrating calixarene derivatives. The calixarene skeleton is devoid of any specificity for cell surface receptors, but the functionalization with homing ligands such as FA may provide it with cancer cell targeting properties. With this in mind, in a previous paper we prepared the first FA-calix[4]arene conjugate, proved its capability to enhance the water solubility of a hydrophobic drug such as indomethacin at physiological pH value, and indicated it as a potential targeted

drug delivery system.[22] In order to make a step towards the demonstration of this potential, in the present work we decided to verify if a folate-calix[4]arene conjugate is able to penetrate FR-positive cells. At this aim we designed and synthesized a fluorescently labeled folate–calix[4]arene conjugate (FA-C4-NBD). The ability of FA-C4-NBD to penetrate cancer HeLa and A375MM cells compared to normal fibroblast NIH3T3 cells, and the intracellular localization in cancer cells were investigated by confocal fluorescence microscopy.

Results and discussion

Design, synthesis and characterization of FA-C4-NBD

For the synthesis of a fluorochrome-labeled folate–calixarene conjugate bearing four folic acid units at the calixarene upper

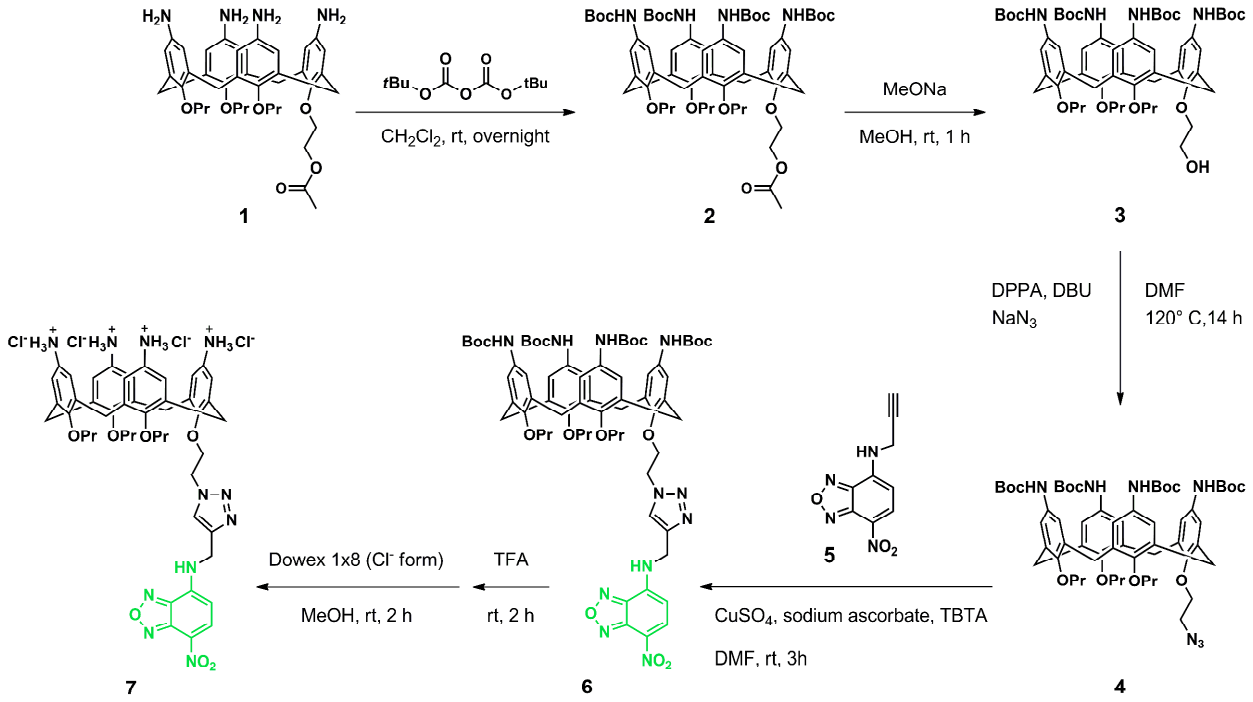

Scheme 1. Synthesis of calix[4]arene-NBD conjugate (**7**).

rim and one fluorochrome moiety at the calixarene lower rim, calixarene derivative **1**,[23] blocked in a cone conformation by the introduction of three propyloxy groups and one acetoxyethoxy group at the calixarene lower rim, was selected as the starting material (Scheme 1). The amino groups of **1** were protected by treatment with di-*tert*-butyl dicarbonate to give compound **2** in 90% yield. Basic hydrolysis of **2** provided the reactive OH group (compound **3**, 95% yield) that was converted in azido group (compound **4**, 66% yield) by treatment with sodium azide, diphenyl phosphoryl azide (DPPA) and 1,8-diazabicyclo[5.4.0.]undec-7-ene (DBU). Compounds **2**-**4** were characterized by 1D and 2D NMR spectroscopy and ESI-MS spectrometry that provided spectral data consistent with the expected structures (See Experimental Section).

Subsequent Cu-catalyzed azide-alkyne cycloaddition (CuCAA, click reaction) between the azido group of **4** and the alkyne group of 7-nitrobenzofurazan (NBD) derivative **5**[24] gave the fluorescent NBD-calixarene derivative **6** in 92% yield (Scheme 1). The introduction of only one fluorochrome group onto the scaffold was planned in order to avoid intramolecular quenching, possible when more fluorescent moieties are in close proximity.[25] The NBD was selected as a fluorochrome because of its known biocompatibility, easy conjugability, and stability inside the cell.[21,26,27] The CuCAA click reaction was choice because it can be carried out in mild reaction conditions and generates a 1,2,3-triazole linker biocompatible and stable to biological environments.[28] The presence of resonances relative to the NBD fluorophore (6.34 and 8.46 ppm for the ArH protons and 7.21 for the NH proton) and triazole ring (7.01 ppm and 124.4 ppm for the CH group) in the ^{1}H- and ^{13}C-NMR spectra of **6** evidenced the success of the click reaction. The structure of **6** was confirmed by the presence of an ion peak at 1322.3 $(M+Na)^{+}$ in the ESI-MS spectrum.

Removal of the Boc groups, by treatment with TFA followed by anionic changing, converted compound **6** in tetra-amino calix[4]arene derivative **7** (chloride salt, 98% yield). Compound **7** (aqueous solution) showed a fluorescence emission band at 549 nm, when excited at 467 nm. Treatment

of compound **7** with 6-azido-hexanoic acid in the presence of benzotriazol-1-yl-oxytripyrrolidinophosphonium hexafluorophosphate (PyBop) and *N,N*-diisopropylethylamine (DIPEA) gave compound **8** in 55% yield (Scheme 2). ^{1}H and ^{13}C-NMR, and ESI-MS spectra of compound **8** corroborated the exhaustive functionalization of the calixarene upper rim (See Experimental Section).

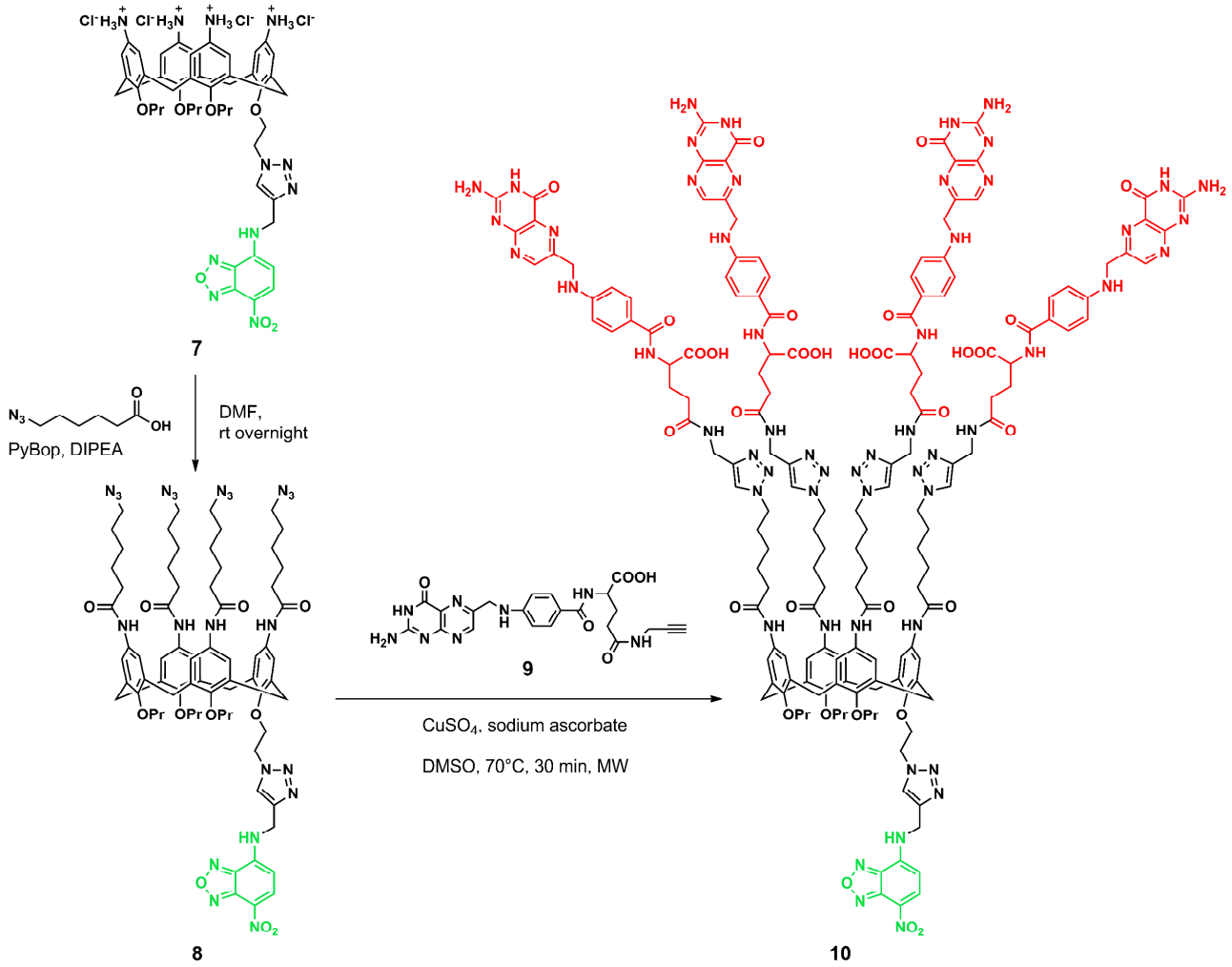

Scheme 2. Synthesis of folate-calix[4]arene-NBD (**10**).

The four azido functionalities of **8** were reacted, by CuCAA reaction, with the alkyne group of the γ-propargyl FA derivative **9**,[29] to afford the designed FA-C4-NBD (**10**) in 47% yield. In compound **10** each FA moiety is linked to the fluorescent calixarene platform by the γ-carboxyl group (Scheme 2). Compound **10** was characterized by 1D- and 2D-NMR spectroscopy, and ESI-MS and MALDI-TOF/TOF-MS spectrometry. The integral ratio between the proton resonances relative to the calixarene macrocycle and the FA residues was consistent with the introduction of four FA units onto the calixarene skeleton. The presence of four FA units in compound **8** was confirmed by an ion peak at 1684.2 $(M + 2H)^{2+}$ in the ESI-MS spectrum and at 3389.3 $(M+Na)^{+}$ in the MALDI-TOF/TOF-MS spectrum. Compound **10** showed a fluorescence emission band at 512 nm, when excited at 488 nm.

A well-defined tridimensional structure in which: (i) four folic acid ligands are arranged on the same side with respect to the mean molecular plane (*all syn* orientation); (ii) each FA ligand is distanced from the calixarene scaffold by a long C6 aliphatic chain which confers flexibility and reduces steric hindrance between the FA ligands; (iii) free folate α-carboxyl groups can preserve a high FA–FRα binding affinity;[30] and (iv) folate pteroate moieties, reported to be buried inside the FRα pocket,[31] stay in terminal position, are structural features that should provide FA-C4-NBD (**10**) with a promising FR binding affinity.

Cellular uptake of FA-C4-NBD

Although the precise mechanism remains not fully resolved and different mechanisms could be involved, it is well documented that folate conjugates can enter cancer cells by FR-mediated

endocytosis[32] and move through cytoplasm organelles.[33] Regarding the calixarene macrocycle, some papers have testified the ability of calixarene derivatives to cross the cell membrane,[34] but at the best of our knowledge never a receptor-mediated cellular uptake mechanism it has been described. A conventional cellular endocytosis was instead ruled out for fluorescent calixarene derivatives.[21,26,35]

The presence of the folate moieties should provide FA-C4-NBD with FR-mediated cell penetration, but this has to be verified since factors such as spacer groups,[36] size[37] and shape[38] of the whole construct can affect the FR binding of multivalent folate-conjugates.

To test if the FA motifs confers to FA-C4-NBD (**10**) the capability to penetrate selectively FR-positive cells via FR-mediated endocytosis, we selected three model cell lines expressing FR at different levels: HeLa, human cervix adenocarcinoma cells (high FR expression levels),[39] NIH3T3, mouse embryonic fibroblast cells (very low FR expression levels)[39,40] and A375MM, a metastatic variant of an established human melanoma cell line (possibly low FR expression levels: data from the parental A375 cell line).[40]

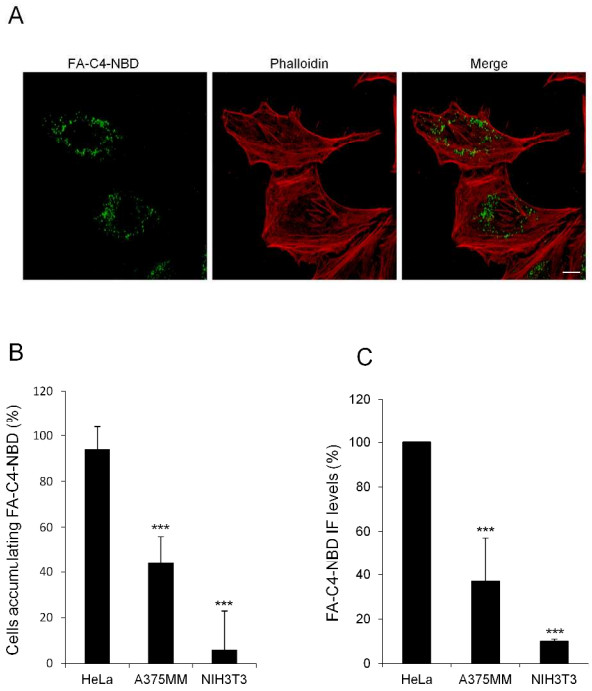

Figure 1. Uptake of FA-C4-NBD in mammalian cells. A. HeLa cells were treated with 10 μM of FA-C4-NBD for 3h, then the excess of FA-C4-NBD was washed out and the cells incubated overnight in standard growth medium. Cells were fixed, permeabilized and stained with Alexa Fluor 543-conjugated phalloidin. Merged images of FA-C4-NBD (green) and phalloidin (red) fluorescence are also shown. Scale bar is 10 μm. B. A375MM cells and NIH3T3 cells were treated as described in A for HeLa cells. The number of HeLa, A375MM and NIH3T3 cells internalizing FA-C4-NBD is shown as percentage of total cells. ***p <0.001, compared to HeLa treated cells (t-test). C. HeLa, A375MM and NIH3T3 cells were treated as in A. The quantification of intracellular FA-C4-NBD IF levels is shown as percentage of the IF in HeLa cells. ***p <0.001, compared to HeLa treated cells (t-test). A-B Data are means ± s.e.m, representative of two independent experiments.

HeLa cells were treated with FA-C4-NBD (10 μM) in complete medium containing 1% of serum, washed to remove the FA-C4-NBD excess and incubated further 24 h in standard growth medium. The cells were fixed, counterstained with phalloidin and analyzed by fluorescent confocal microscopy. More than 95% of the treated HeLa cells showed FA-C4-NBD fluorescence which appears mostly as intracellular dots-like structures, sometimes a small fluorescent pattern compatible with plasma membrane localization was also observed (Figures 1A and B).

A375MM and NIH3T3 cells treated with FA-C4-NBD, as described above for HeLa cells, presented the dot like accumulation of fluorescence only in about 45% of A375MM cells and 5% of NIH3T3 cells (Figure 1B). This result indicated that, FA-C4-NBD might enter the cells using the FR as a shuttling mechanism. Later on, we selected those cells that accumulated FA-C4-NBD and quantitated the intracellular fluorescence levels. As shown in figure 1C, the amount of internalized FA-C4-NBD was completely different among the three cell lines. Specifically, the quantity of FA-C4-NBD internalized in A375MM and NIH3T3 cells was only 37% and 10% of that internalized by HeLa cells. Note that the amount of intracellular FA-C4-NBD nicely correlates with the expression levels of FR. Our data are in line with previous reports showing that HeLa cells expressing a higher amount of functional FR, internalize folate conjugates more efficiently than NIH3T3 cells, which express lower levels of FRs.[38] The parallel experiments performed on HeLa, A375MM, and NIH3T3 cells provided preliminary information about the cell-type specificity of FA-C4-NBD internalization.

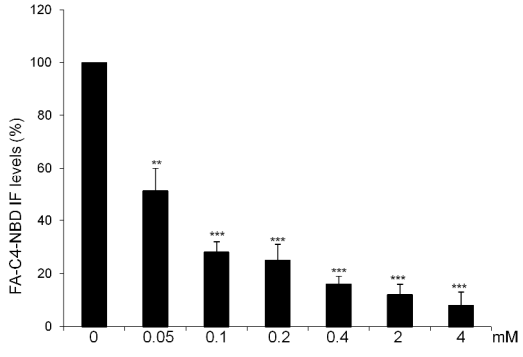

Figure 2. Free folic acid compete for the uptake of FA-C4-NBD in mammalian cells. HeLa cells were incubated for 30 minute with the indicated doses of folic acid, then treated with 10 μM of FA-C4-NBD for 3h, always in the presence of the same concentration of folic acid. The excess of FA-C4-NBD was washed out and the cells incubated overnight in standard growth medium. Cells were fixed and FA-C4-NBD fluorescence analyzed by fluorescent microscopy. The quantification of intracellular fluorescence levels of FA-C4-NBD is shown. Data are means ± s.e.m, representative of two independent experiments, and they are expressed as percentage of fluorescence in HeLa cells not incubated with free folic acid. *** p <0.001, ** p<0.01, compared to control HeLa cells not incubated with free folic acid (ANOVA analysis).

To further validate the role of FR in the FA-C4-NBD uptake we carried out competition experiments with free FA. This is a

method designed to saturate FRs and prevent FR-specific binding by folate conjugates, there-by distinguishing between receptor-mediated and non-specific uptake.[41]

HeLa cells were pre-treated with different concentration of free FA for 30 min before the addition of FA-C4-NBD for further 3 h, then the cells were washed, fixed and analyzed for the presence of FA-C4-NBD fluorescence. Pre-incubation of free FA reduced the amount of FA-C4-NBD internalized in a concentration dependent manner (Figure 2). Remarkably, a 4 mM concentration of free FA (about 400-fold excess) was required to substantially block the uptake of 10 μM FA-C4-NBD in HeLa cells (Figure 2). These data supported that free FA and FA-C4-NBD compete for the FR binding and corroborated the FR-mediated cell penetration of FA-C4-NBD. Differently from FA-C4-NBD, an analogous amino-calix[4]arene-NBD conjugate lacking in the FA ligands is not taken into the cells via an active endocytosis,[26] this further supports the role of the FA ligands in the cellular uptake of FA-C4-NBD.

Considering the hydrophobic nature of both calixarene scaffold and FA moieties, it cannot be excluded that FA-C4-NBD can form aggregates in physiological medium. Preliminary dynamic light scattering measurements carried out on a sample of FA-C4-NBD in PBS at pH 7.4, showed the presence of aggregates with hydrodynamic diameter 137 ± 37 nm, and polydispersity index 0.3. It is hypothesizable an aggregate structure in which some FA moieties refuge water but a number of FA ligands higher than the four units of the monomeric structure is exposed on the aggregate surface suitable to interact with the FRs on the cell surface. The formation of aggregates induced by folate residues and the ability of these aggregates to enter FR positive cells were described for HPMA–folate conjugates.[14]

Intracellular localization of FA-C4-NBD

Chemical compounds internalized into eukaryotic cells *via* receptor-mediated endocytosis can follow different intracellular routes, accumulate into the endo-lysosomal compartment, travel towards the Golgi complex or recycle back outside the cells. The tubule-vesicular structures primarily formed along the endocytosis pathway are characterized by the presence of the early endosome antigen 1 (EEA1) and the small G protein Rab5.[42]

The sorting from this early endosomes into late endosomes/lysososmes can be detected by the colocalization with the lysosome associated membrane protein 1 (LAMP1).[43] The sorting toward the recycling route involves the incorporation of cargoes into Rab11 positive endosomes.

Finally, the sorting towards the Golgi can be revealed by the colocalization with the Golgi marker GM130.

HeLa cells were treated with FA-C4-NBD as described above, fixed, counterstained with specific organelle markers and analyzed by fluorescent confocal microscopy. FA-C4-NBD did not reach the Golgi complex as shown by the low colocalization with the Golgi marker GM130 (Figure 3A and B).

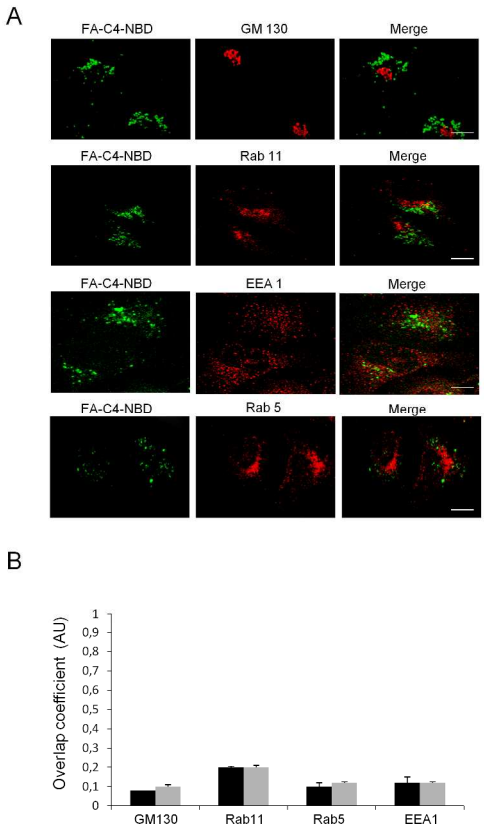

Figure 3. Analysis of intracellular localization of FA-C4-NBD in mammalian cells. A. HeLa cells were treated with 10 μM of FA-C4-NBD for 3h, then the excess of FA-C4-NBD was washed out and the cells incubated overnight in standard growth medium. Cells were fixed, permeabilized and stained with the indicated organelle markers. Merged images of FA-C4-NBD (green) and organelle markers (red) fluorescence are also shown. Scale bar is 10 μm. B. Quantification of FA-C4-NBD fluorescence colocalizing with the organelle markers shown in A. Black bars indicate the extent of FA-C4-NBD overlapping with the organelle marker. Gray bars indicate the extent of organelle marker overlapping with FA-C4-NBD. Data are means of overlapping coefficient ± s.e.m, representative of two independent experiments. AU: arbitrary units.

The FA-C4-NBD fluorescence was also negligible inside the early endosomes and the recycling endosome as shown by the low colocalization with EEA1, Rab5 and Rab11, (Figure 3A and B). Remarkably, intracellular FA-C4-NBD mainly colocalized with lysosomal marker LAMP1 (Figure 4A and B). Note that FA-C4-NBD accumulates in the lysosomal compartment also in A375MM cells (not shown).

Finally, to further validate the involvement of the endocytic pathway to the uptake of FA-C4-NBD, HeLa cells were treated for 1 hour with FA-C4-NBD, fixed and counterstained with EEA1 and LAMP1. FA-C4-NBD was seen in the early endosome as judged by a distinct colocalization with the endosome marker EEA1, although, we could appreciate a minor colocalization with the lysosomal marker LAMP1 (Figure 4C and D). These data suggest that FA-C4-NBD is internalized and accumulates into the lysosome of HeLa cells by travelling along the endocytic pathway.

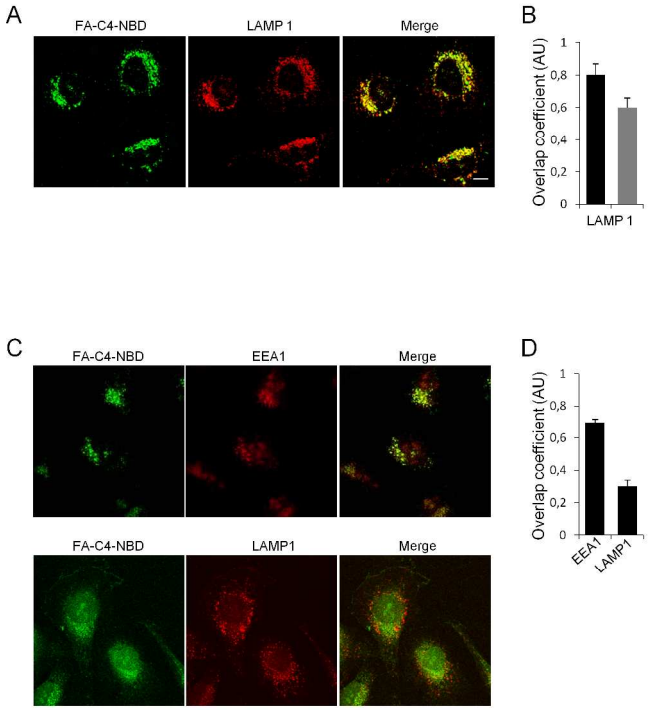

Figure 4. FA-C4-NBD is localized to the lysosomal compartment. A. HeLa cells were treated with 10 µM of FA-C4-NBD for 3h, then the excess of FA-C4-NBD was washed out and the cells incubated over night in standard growth medium. Cells were fixed, permeabilized and stained with LAMP1. Merged images of FA-C4-NBD (green) and LAMP1 (red) fluorescence are also shown. Scale bar is 10 µm. B. Quantification of FA-C4-NBD fluorescence colocalizing with LAMP1. Black bar indicates the extent of FA-C4-NBD overlapping with LAMP1. Gray bar indicates the extent of LAMP1 overlapping with FA-C4-NBD. Data are means of overlapping coefficient ± s.e.m, representative of two independent experiments. C. HeLa cells were treated with 10 µM of FA-C4-NBD for 1h, then immediately fixed, permeabilized and stained with EEA1 and LAMP1. D. Quantification of FA-C4-NBD fluorescence colocalizing with EEA1 or LAMP1 as indicated. Data are means of overlapping coefficient ± s.e.m, of a representative experiment. AU: arbitrary units.

The accumulation of FA-C4-NBD in lysosomes agrees with other researches reporting that folate derivatives, such as folate conjugated to albumin,[44] single walled carbon,[45] HPMA polymer,[14] and nanoparticle,[46] enter the cell via FR-mediated endocytosis and localize in lysosomes.

Experimental Section

Materials. All chemicals and solvents were of reagent quality and used without further purification unless otherwise stated. Analytical TLCs were performed on 0.25 mm silica gel 60 coated aluminium foils with F-254 indicator (Merck). Preparative TLCs were carried out on silica gel plates (Kieselgel 60 F254, 1 mm, Merck). Column chromatography was performed on silica gel (Kieselgel 60, 63-200 µm, Merck) or on Sephadex LH-20. Dowex 1x8 chloride was purchased from Sigma-Aldrich.

All buffer components were of biological grade. Anti-EEA1 was from Santa Cruz Biotechnology; anti-GM130, anti-Rab5 and anti-Rab11 were from BD transduction Laboratories; anti-LAMP1 was from Abcam; Alexa-543-conjugated Phalloidin, Alexa-543-conjugated secondary antibodies were from Invitrogen. All the culture medium, serum and PBS were from Invitrogen.

Instrumentation. ^{1}H NMR (400.13 MHz), ^{13}C NMR (100.61 MHz), and 2D-NMR spectra were acquired on a Bruker Avance^{TM} 400 spectrometer. Chemical shifts (δ) are expressed in parts per million (ppm), and reported relative to the residual proton solvent peaks; coupling constant (J) values are given in Hz. Mass spectra were acquired on a Waters Micromass ZQ 2000 spectrometer, electrospray ionization probe (positive ion mode) or an Applied Biosystems 4800 MALDI TOF/TOF Analyzer instrument equipped with a Nd:YAG laser with 355 nm wavelength of <500 ps pulse and 200 Hz repetition rate (reflector positive ion mode). Fuorescence spectra were recorder on a Fluoromax-3 from Horiba-Jobin-Yvon fluorescence spectrometer. Particle size and polydispersity index were measured for a colloidal dispersion of compound **10** (20 µM) in PBS, at pH 7.4 and 25 °C by photon correlation spectroscopy using a Zetasizer Nano ZS-90 Malvern Instrument (Malvern, UK). Immunofluorescence confocal images were acquired using a Zeiss Pascal inverted confocal microscope system (Carl Zeiss, Gottingen, Germany). Fixed cells were analysed using a 63× oil-immersion objective, maintaining the pinhole of the objective at 1 Airy unit. Images were acquired under non-saturating conditions (pixel fluorescence below 255 arbitrary units) and using the same settings for all samples.

Syntheses of compounds 1-10. Starting compound *5,11,17,23-tetra-amino-25,26,27-tripropoxy-28-(2-acetoxyethoxy)-calix[4]arene* (**1**) was prepared by following the synthetic protocol previously reported.[23]

5,11,17,23-Tetra-Boc-amino-25,26,27-tripropoxy-28-(2-acetoxyethoxy)-calix[4]arene (**2**). To compound **1** (200 mg, 0.29 mmol) dissolved in passed through basic alumina CH_2Cl_2 (8 mL), di-*tert*-butyl dicarbonate (0.33 mL, 1.44 mmol) was added. The mixture was stirred at rt overnight, then a 5% aq $NaHCO_3$ solution (50 mL) and CH_2Cl_2 (50 mL) were added. Organic phase was washed with 5% aq $NaHCO_3$ solution (50 mL) and water (50 mL × 2). After removal of the solvent under vacuum, the solid residue was washed with hexane and recovered by filtration to give pure compound **2** (283 mg, 90%). ^{1}H NMR ($CDCl_3$, 297 K) δ: 0.91 (t, J = 7.4 Hz, 3H, propyl CH_3), 0.96 (t, J = 7.4 Hz, 6H, 2 × propyl CH_3), 1.47, 1.50 (s, 18H each, 4 × Boc CH_3), 1.84 (m overlapped, 6H, 3 × propyl CH_2CH_3), 2.00 (s, 3H, $COCH_3$), 3.09 and 4.37 (AX system, J = 13.4 Hz, 2H, $ArCH_2Ar$), 3.10 and 4.35 (AX system, J = 13.4 Hz, 2H, $ArCH_2Ar$), 3.71 (t, J = 7.4 Hz, 4H, 2 × propyl $CH_2CH_2CH_3$), 3.80 (t, J = 7.4 Hz, 2H, propyl $CH_2CH_2CH_3$), 4.14 (t, J = 5.1, Hz, 2H, CH_2CH_2OAc), 4.50 (t, J = 5.5, Hz, 2H, CH_2CH_2OAc), 6.04 (s, 2H, 2 × NH), 6.23 (s, 2H, 2 × NH), 6.45, 6.46 (s, 2H each, 4 × ArH), 6.77 (s, 4H, 4 × ArH). ^{13}C NMR ($CDCl_3$, 297 K) δ: 10.1, 10.3, 20.8 (q), 22.9, 23.0 (t), 28.3 (q), 30.9, 64.2, 71.7, 77.3 (t), 79.8, 79.9 (s), 119.6, 119.9, 120.0 (d), 131.9, 132.0, 132.4 (s), 134.4, 134.5, 135.4, 135.6 (d), 152.4, 152.8, 152.9, 153.2, 153.4, 170.8 (s). ESI-MS (m/z): calcd for $C_{61}H_{84}N_4NaO_{14}$ $(M + Na)^+$ 1119.6, found 1120.5; for $C_{61}H_{84}KN_4O_{14}$ $(M+K)^+$ 1135.6, found 1136.4.

5,11,17,23-Tetra-Boc-amino-25,26,27-tripropoxy-28-(2-hydroxyethoxy)-calix[4]arene (**3**). Compound **2** (250 mg, 0.23 mmol) was dissolved in 0.5 N MeONa (4.5 mL) and stirred at rt for 1h. Amberlite IRC-50® (H^+) ion-exchange resin was added to neutralize the base excess until pH 6. The mixture was stirred at room temperature for 10 min, the solid was filtered off and washed with MeOH. The collected filtrate was evaporated *in vacuo* to give pure compound **3** (229 mg, 95%). ^{1}H NMR ($CDCl_3$, 297 K) δ: 0.84 (t, J = 7.4 Hz, 3H, propyl CH_3), 0.99 (t, J = 7.4 Hz, 6H, 2 × propyl CH_3), 1.43, 1.54 (s, 18H each, 4 × Boc CH_3), 1.86 (m overlapped, 6H, 3 × propyl CH_2CH$_3$), 3.09 and 4.37 (AX system, J = 13.4 Hz, 2H, ArCH_2Ar), 3.13 and 4.27 (AX system, J = 13.4 Hz, 2H, ArCH_2Ar), 3.62 (t, J = 7.4 Hz, 4H, 2 × propyl CH_2CH$_2$CH$_3$), 3.90 (br t, 2H, CH_2OH), 3.98 (br t, 2H, CH_2CH$_2$OH), 4.03 (t, J = 7.4 Hz, 2H, propyl CH_2CH$_2$CH$_3$), 4.91 (t, J = 6.5, Hz, 1H, CH$_2$O*H*), 5.89 (s, 2H, 2 x NH), 6.16 (s, 4H, 4 × ArH), 6.46 (s, 2H, 2 x NH), 7.14, 7.16 (s, 2H each, 4 × ArH). ^{13}C NMR ($CDCl_3$, 297 K) δ: 9.8, 10.5 (q), 22.3, 23.0 (t), 28.4 (q), 30.8, 30.9, 61.2, 77.7 (t), 79.9, 80.1, 80.2 (s), 119.1, 119.3, 120.3, 120.5 (d), 132.2, 132.4, 133.0 (s), 133.2, 133.4, 136.8, 136.9 (d), 150.9, 152.8, 153.0, 153.1, 153.5 (s). ESI-MS (*m*/*z*): calcd for $C_{59}H_{82}N_4NaO_{13}$ $(M + Na)^+$ 1077.6, found 1078.2.

5,11,17,23-Tetra-Boc-amino-25,26,27-tripropoxy-28-(2-azidoethoxy)-calix[4]arene (**4**). A mixture of calixarene derivative **3** (200 mg, 0.19 mmol), sodium azide (99 mg, 1.52 mmol), diphenyl phosphoryl azide (246 µL, 1.14 mmol), 1,8-diazabicyclo[5.4.0.]undec-7-ene (114 µL, 0.76 mmol) and anhydrous DMF (2.5 mL) was stirred at 120 °C for 14 h. The reaction mixture was cooled to room temperature, diluted with Et_2O (80 mL), washed with H_2O (2 × 10 mL). The organic phase was dried with anhydrous Na_2SO_4 and concentrated under vacuum. Pure compound **4** (135 mg, 66%) was obtained after column chromatography with hexane/AcOEt as eluent (gradient 95:5 to 70:30, *v*/*v*). ^{1}H NMR ($CDCl_3$, 297 K) δ: 0.92 (t, J = 7.6 Hz, 3H, propyl CH_3), 1.00 (t, J = 7.6 Hz, 6H, 2 × propyl CH_3), 1.45, 1.51 (s, 18H each, 4 × Boc CH_3), 1.85 (m overlapped, 6H, 3 × propyl CH_2CH$_3$), 3.09 and 4.37 (AX system, J = 13.4 Hz, 2H, ArCH_2Ar), 3.13 and 4.30 (AX system, J = 13.4 Hz, 2H, ArCH_2Ar), 3.69 (t, 4H, 2 × propyl CH_2CH$_2$CH$_3$), 3.80-3.86 (overlapped, 4H, propyl CH_2CH$_2$CH$_3$ and CH_2CH$_2$N$_3$), 4.05 (t, 2H, J = 6.8 Hz, CH$_2$CH_2N$_3$), 6.03 (s, 2H, 2 x ArNH), 6.31 (s, 2H, 2 x ArNH), 6.37 (s, 4H, 4 × ArH), 6.88 (d, 4H, 4 × ArH). ^{13}C NMR ($CDCl_3$, 297 K) δ: 10.0, 10.5 (q), 22.9, 23.2 (t), 28.4 (q), 30.9, 31.0, 50.7 (t), 80.0, 80.1, 80.2 (s), 119.5, 119.6, 120.0, 120.2 (d), 132.0, 132.2, 132.8, 134.1, 134.3, 135.8, 136.0, 152.1, 152.5, 153.0, 153.1 (s). ESI-MS (*m*/*z*): calcd for $C_{59}H_{81}N_7NaO_{12}$ $(M + Na)^+$ 1102.6, found 1103.3.

5,11,17,23-Tetra-Boc-amino-25,26,27-tripropoxy-28-{2-[4-((7-Nitrobenzofurazan-4-yl)aminomethyl)-triazol-1-yl]ethoxy}-calix[4]arene (**6**). A mixture of calixarene derivative **4** (130 mg, 0.12 mmol), 7-nitro-4-(prop-2-ynylamino)benzofurazan **5**[24] (33 mg, 0.15 mmol), $CuSO_4$•5 H_2O (1.3 mg, 5.2 µmol), sodium ascorbate (7.9 mg, 40 µmol) and tris[(1-benzyl-1*H*-1,2,3-triazol-4-yl)methyl]amin (TBTA, 2.7 mg, 5.1 µmol) in anhydrous DMF (2.5 mL) was stirred under argon at rt for 3 h. The reaction mixture was evaporated to dryness to give a residue, which was purified by column chromatography with CH_2Cl_2/AcOEt as eluent (95:5, *v*/*v*) to afford compound **6** (144 mg, 92%) as an orange powder. ^{1}H NMR ($CDCl_3$, 297 K) δ: 0.87 (t, J = 7.4 Hz, 3H, propyl CH_3), 0.98 (t, J = 7.4 Hz, 6H, 2 × propyl CH_3), 1.44 (s, 18H, 2 × Boc CH_3), 1.52, 1.53 (s, 9H each, 2 × Boc CH_3), 1.83 (m overlapped, 6H, 3 × propyl CH_2CH$_3$), 3.03 and 4.11 (AX system, J = 13.4 Hz, 2H, ArCH_2Ar), 3.10 and 4.36 (AX system, J = 13.4 Hz, 2H, ArCH_2Ar), 3.63 (m, 4H, 2 × propyl CH_2CH$_2$CH$_3$), 3.89 (t, J = 7.4 Hz, 2H, propyl CH_2CH$_2$CH$_3$), 4.53 (t, J = 6.2 Hz, 2H, CH_2CH$_2$N), 4.75 (d, J = 5.4 Hz, 2H, CH_2NH), 4.92 (t, J = 6.3 Hz, 2H, CH$_2$CH_2N), 5.98 (s, 2H, 2 × ArNH), 6.24, 6.26 (s, 2H each, 4 × calixarene ArH), 6.34 (d, 1H, J = 8.6 Hz, probe ArH), 6.40 (s, 1H, calixarene ArNH), 6.43 (s, 1H, calixarene ArNH), 6.89, 6.99 (s, 2H each, 4 × calixarene ArH), 7.01 (s, 1H, triazole CH), 7.25 (overlapped chloroform, 1H, ArN*H*CH$_2$), 8.46 (d, 1H, J = 8.6 Hz, probe ArH). ^{13}C NMR ($CDCl_3$, 297 K) δ: 10.0, 10.5 (q), 22.9, 23.2 (t), 28.0, 28.3, 28.6 (q), 30.8, 31.0, 39.2, 50.5, 70.7 (t), 79.9, 80.2, 80.5 (s), 99.0, 119.3, 119.8, 120.3, 121.1 (d), 121.8 (s), 124.4 (d), 132.1, 132.4, 132.7, 133.2, 133.8, 136.1, 142.0, 143.8, 144.2, 151.7, 152.2, 153.0, 153.1, 153.4, 153.7 (s). ESI-MS (*m*/*z*): calcd for $C_{68}H_{87}N_{11}NaO_{15}$ $(M + Na)^+$ 1320.6, found 1322.3; calcd for $C_{68}H_{87}N_{11}KO_{15}$ $(M + K)^+$ 1336.6, found 1338.4

5,11,17,23-Tetra-amino-25,26,27-tripropoxy-28-{2-[4-((7-Nitrobenzofurazan-4-yl)aminomethyl)-triazol-1-yl]ethoxy}-calix[4]arene (**7**). Compound **6** (140 mg, 0.11 mmol) was dissolved in TFA (2.5 mL) and stirred at rt for 2 h. The reaction mixture was evaporated to dryness, dissolved in EtOH and evaporated to remove all traces of TFA. The solid was dissolved in MeOH and stirred in the presence of Dowex 1x8 chloride form excess for 2 h. The filtrate was evaporated to afford de-Boc compound **7** as a chloride salt (110 mg, 98%). ^{1}H NMR (MeOD, 297 K) δ: 0.91 (t, J = 7.4 Hz, 6H, 2 × propyl CH_3), 1.00 (t, J = 7.4 Hz, 3H, propyl CH_3), 1.77 (m, J = 7.4 Hz, 4H, 2 × propyl CH_2CH$_3$), 1.86 (m, J = 7.4 Hz, 2H, propyl CH_2CH$_3$), 3.21 and 4.18 (AX system, J = 13.6 Hz, 2H, ArCH_2Ar), 3.26 and 4.44 (AX system, J = 13.6 Hz, 2H, ArCH_2Ar), 3.60-3.78 (m, 4H, 2 × propyl CH_2CH$_2$CH$_3$), 3.82 (t, J = 7.4 Hz, 2H, propyl CH_2CH$_2$CH$_3$), 4.45 (overlapped t, 2H, CH_2CH$_2$N), 4.75 (overlapped H_2O, 2H, CH_2NH), 4.92 (overlapped H_2O, 2H, CH$_2$CH_2N), 6.46 (d, J = 8.8 Hz, 1H, probe ArH), 6.55, 6.59, 6.79, 6.86 (s, 2H each, 8 x ArH), 8.19 (s, 1H, triazole CH), 8.34 (d, 1H, J = 8.8 Hz, probe ArH).^{13}C NMR (MeOD, 297 K) δ: 10.6, 10.8 (q), 24.3, 31.5, 39.2, 51.0, 71.2, 77.1, 78.5 (t), 102.9, 123.9, 124.1, 124.2, 124.4, 124.6 (d), 125.5, 126.2, 126.9, 135.5, 137.2, 137.5, 137.7 (s), 138.1 (d), 142.1, 145.8, 156.5, 157.1, 157.7 (s). ESI-MS (*m*/*z*): calcd for $C_{48}H_{56}N_{11}O_7$ $(M + H)^+$ 898.4, found 898.2; calcd for $C_{48}H_{55}N_{11}NaO_7$ $(M + Na)^+$ 920.4, found 920.5.

5,11,17,23-Tetra-(6-azidohexanoyl)amino-25,26,27-tripropoxy-28-{2-[4-((7-Nitrobenzofurazan-4-yl)aminomethyl)-triazol-1-yl]ethoxy}-calix[4]arene (**8**). To a stirred solution of 6-azido-hexanoic acid (90 mg, 0.57 mmol), PyBop (390 mg, 0.75

mmol) and DIPEA (300 µL, 1.72 mmol) in dry DMF (10 mL), a solution of compound **7** (100 mg, 0.096 mmol) and DIPEA (134 µL, 0.77 mmol) in dry DMF (5 mL) was added. The stirring was continued at rt overnight. The solvent was removed under vacuum and the residue was washed with 0.1 N HCl and water. Purification by preparative TLC (100% AcOEt) provided pure compound **8** (77 mg, 55%) as an orange powder. ^{1}H NMR (MeOD, 297 K) δ: 0.91 (t, *J* = 7.4 Hz, 3H, propyl CH_3), 0.95 (t, *J* = 7.4 Hz, 3H, 2 × propyl CH_3), 1.41 (m, *J* = 7.4 Hz, 8H, 4 × hexanoyl $CH_2CH_2CH_2N_3$), 1.61 (overlapped m, 16H, 4 × hexanoyl $CH_2CH_2N_3$ and 4 × hexanoyl $CH_2CH_2CH_2CH_2N_3$), 1.85 (overlapped m, 6H, 3 × propyl CH_2CH_3), 2.21 and 2.28 (t, *J* = 7.4 Hz, 4H each, 4 × hexanoyl $COCH_2$), 3.02 and 4.18 (AX system, *J* = 13.2 Hz, 2H, $ArCH_2Ar$), 3.08 and 4.41 (AX system, *J* = 13.2 Hz, 2H, $ArCH_2Ar$), 3.27 (overlapped methanol, 8H, 4 × hexanoyl CH_2N_3), 3.66 (t, *J* = 7.2 Hz, 4H, 2 × propyl $CH_2CH_2CH_3$), 3.87 (t, *J* = 7.2 Hz, 2H, propyl $CH_2CH_2CH_3$), 4.45 (t, *J* = 6.6 Hz, 2H, CH_2CH_2N), 4.75 (s, 2H, CH_2NH), 5.00 (t, *J* = 6.6 Hz, 2H, CH_2CH_2N), 6.40 (d, *J* = 8.8 Hz, 1H, probe ArH), 6.39, 6.41, 6.69, 6.73 (s, 2H each, calixarene 8 × ArH), 7.98 (s, 1H, triazole CH), 8.37 (d, 1H, *J* = 8.8 Hz, probe ArH). ^{13}C NMR (MeOD, 297 K) δ: 10.6, 10.9 (q), 24.3, 24.4, 26.3, 26.4, 27.5, 29.7, 31.9, 32.1, 37.6, 51.5, 52.3, 72.7, 78.4 (t), 102.9, 121.7, 121.9, 122.0 (d), 122.2 (s), 124.3 (d), 133.7, 133.8, 134.5, 135.2, 135.6, 136.4, 136.5 (s), 138.0 (d), 144.7, 145.3, 145.9, 153.5, 153.7, 154.5, 173.7, 173.9 (s). ESI-MS (*m/z*): calcd for $C_{72}H_{91}N_{23}NaO_{11}$ $(M + Na)^+$ 1476.7, found 1477.8.

Compound 10 (*FAC4NBD*). To a solution of compound **8** (10 mg, 6.9 µmol) and γ-propargyl folate **9**[29] (26 mg, 54 µmol) in dry DMSO (350 µL), $CuSO_4$•5 H_2O (1.5 mg, 6.0 µmol) and sodium ascorbate (7.7 mg, 39 µmol) were added. The mixture was stirred in a 10 mL closed vessel at 70 °C into a microwave apparatus for 30 min. The reaction was stopped by adding cold acetone (2 mL). A precipitate was formed which was collected by centrifugation at 3000 rpm for 5 min. The solid was washed with CH_2Cl_2 (2 mL) and CH_3CN (2 mL), then was suspended in water (2 mL) and 0.1 N HCl was added until to pH 5. The precipitate was collected by centrifugation and washed by CH_3CN (2 mL) and Et_2O (2 mL), and dried *in vacuo*. The crude product was dissolved in aqueous 0.1 N NaOH/MeOH (9:1) and purified by gel permeation on Sephadex LH-20 (eluent 9:1 H_2O/MeOH). A yellow precipitate was formed by adding 0.1 N HCl to the collected fractions until pH 5. After centrifugation the solid was washed with CH_3CN (2 mL) and Et_2O (2 × 2 mL) to afford pure compound **10** (11 mg, 47% yield) as an orange powder. ^{1}H-NMR (DMSO-d_6, 297 K): δ 0.82 (t, *J* = 6.8 Hz, 9H, 3 × propyl CH_3), 1.16, 1.22 (overlapped m, 8H, 4 × hexanoyl $CH_2CH_2CH_2N$), 1.47, 1.54 (overlapped m, 8H, 4 × hexanoyl $CH_2CH_2CH_2CH_2N$), 1.30-1.42 (overlapped m, 14H, 4 × hexanoyl CH_2CH_2N, 3 × propyl CH_2CH_3), 1.89 and 2.07 (m, 4H each, 4 × glutamyl $CHCH_2$), 2.00-2.40 (overlapped, 16H, 4 × glutamyl CH_2CO and 4 × hexanoyl $COCH_2$), 3.04 (d, *J* = 12.0 Hz, 4H, 2 × $ArCH_2Ar$), 3.58 (br t, 4H, 2 × propyl $CH_2CH_2CH_3$), 3.83 (br t, 2H, propyl $CH_2CH_2CH_3$), 4.10-4.35 (overlapped, 26H, CH_2CH_2N, 4 × hexanoyl CH_2N, 2 × $ArCH_2Ar$, 4 × glutamyl CH, 4 × triazole CH_2NHCO), 4.46 (s, 8H, 8 × pteroyl CH_2NH), 4.76 (br s, 2H, probe CH_2NH), 4.97 (br s, 2H, CH_2CH_2N), 6.49 (d, *J* = 8.9 Hz, 1H, probe ArH), 6.61 (d, *J* = 8.1 Hz, 8H, 8 × pteroyl ArH), 6.75 (s, 4H, 4 × calixarene ArH), 6.85-7.02 (overlapped, 12H, pteroyl NH_2, pteroyl CH_2NH), 7.08 (s, 4H, 4 × calixarene ArH), 7.63 (d, *J* = 8.1 Hz, 8H, 8 × pteroyl ArH), 7.82, 7.84 (s, 2H each, 4 × triazole CH), 8.18 (s, 1H, triazole CH), 8.19 (d, J = 7.0 Hz, 4H, 4 × glutamyl CHNH), 8.33 (br t, 4H, 4 × $CONHCH_2$), 8.46 (d, *J* = 8.9 Hz, 1H, probe ArH), 8.62 (s, 4H, 4 × pteroyl NCH), 9.32, 9.56 (br s, 2H each, 4 × calixarene ArNH), 9.88 (br t, 1H, probe CH_2NH). ^{13}C-NMR (DMSO-d6, 297 K): 11.9, 12.2 (q), 24.6, 26.4, 27.6, 28.4, 31.6, 32.8, 33.8, 36.2, 37.9, 47.9, 51.1 (t), 52.1 (d), 74.9, 78.8 (t), 102.1, 113.2, 121.4, 121.5, 123.3, 124.5, 124.8 (d), 129.9, 130.3 (s), 130.9 (d), 135.1, 135.2, 135.4, 136.6, 136.7, 139.1, 146.8 (s), 150.6 (d), 151.7, 150.7, 152.9, 155.7, 162.9, 168.4, 172.3, 172.4, 172.5, 173.5, 175.8 (s). ESI-MS m/z calcd for $C_{160}H_{181}N_{55}O_{31}^{2+}$ $(M + 2H)^{2+}$ 1684.2, found 1684.2; MALDI-TOF/TOF-MS m/z calcd for $C_{160}H_{179}N_{55}NaO_{31}$ 3389.4 $(M + Na)^+$, found 3389.3.

Cell culture. HeLa, A375MM and NIH3T3 cells were grown under standard condition as described in literature.[47,48] Briefly, HeLa, and NIH3T3 cells were grown in Dulbecco's Modified Eagle Medium (DMEM), while A375MM cells were grown in DMEM-F12, both medium were supplemented with 2 mM glutamine, 100 U/ml penicillin, 100 µg/ml streptomycin, 10% FCS and maintained at 37 °C in a controlled humidified atmosphere containing 5% CO_2.

Cellular uptake of FA-C4-NBD. About 800.000 cells were plated in complete medium on coverslips placed in 24 well plate (70-80% of confluence). The day after the cells were washed three times in serum-free medium and incubated with 10 µM of NBD-C4-FA as indicate in the figures in growth medium containing 1% FCS. The incubation was carried out at 37 °C for 3 hours. Cells were then washed three times with medium containing 1% of FCS and incubated overnight in complete medium at 37 °C in a controlled humidified atmosphere containing 5% CO2. The day after the cells were washed in HBSS containing calcium and magnesium, fixed in 4% of paraformaldehyde for 8-10 min at 37 °C, and processed for immunofluorescence as previously described.[47] The competition with free folate (the concentrations are indicated in the figure) was carried out by pre-incubating the cells 30 min before the addition of NBD-C4-FA and remained in the culture medium during the 3 hours of incubation with NBD-C4-FA. The rest of the procedure was identical to the described uptake of NBD-C4-FA without folate competitor.

Quantification of fluorescence signals. Immunofluorescence microscopy was performed as previously described.[48] The fluorescent spots was delineated manually and fluorescence intensity quantified using the LSM510-3.2 software (Zeiss). The total fluorescence for each condition was subtracted by background and normalised for cell number. All experiments

were carried out at least twice. To assess the colocalization we removed the background immunofluorescence by adjusting the threshold levels and used the histo and colocalization functions of the LSM510-3.2 software (Zeiss). The coefficient quantifying the colocalization overlap is expressed in arbitrary unit.

Conclusions

In summary, for the first time a calix[4]arene scaffold has been engineered to perform a receptor-mediated cell penetration. At this aim, four folate groups as homing ligands have been tethered to the calix[4]arene skeleton previously conjugated to a NBD fluorochrome to give a multivalent fluorescent folate–calixarene conjugate (FA-C4-NBD). Our data indicate that the folate ligands arranged onto the calix[4]arene scaffold maintain folate receptor binding affinity and drive the cellular uptake of the fluorescent folate–calix[4]arene conjugate. The negligible penetration of normal NIH3T3 cells over folate receptor richer cancer HeLa cells, the competition with free folic acid, and the co-localization with endo-lysosomal markers, support a model where the folate–calixarene conjugate enters selectively cancer cells over health cells via FR-mediated endocytosis. The here reported results open perspectives for using the multifunctionalizable calixarene macrocycles as novel platforms that combining targeting ligands with drugs and/or diagnostics may provide a wide variety of novel targeted delivery systems also attractive for theranostics and multidrug therapy.

Acknowledgements

We would like to thank the Italian Association for Cancer Research, AIRC (Italy). This study was supported by an AIRC Grant n. IG 11652 (to MS). M. Grossi was a recipient of a Fellowship from Fondazioni per il Sud.

Notes and references

[a] Istituto di Chimica Biomolecolare, C.N.R., Via Paolo Gaifami 18, I-95126, Catania, Italy.
[b] Unit of Genomic Approaches to Membrane Traffic, Fondazione Mario Negri Sud, Via Nazionale 8/A, 66030, S. Maria Imbaro (CH), Italy.

*Corresponding Authors
Email: grazia.consoli@icb.cnr.it; Tel: +39-095-7338319
Email: sallese@negrisud.it; Tel: +39-087-2570421

Electronic Supplementary Information (ESI) available: NMR, fluorescence, and DLS spectra. See DOI: 10.1039/b000000x/

1. H. Elnakat and M. Ratnam, *Adv. Drug Deliv. Rev.*, 2004, **56**, 1067.
2. I. R. Vlahov and C. P. Leamon, *Bioconjugate Chem.*, 2012, **23**, 1357.
3. H.-M. Yang, C. W. Park, P. K. Bae, T. Ahn, B.-K. Seo, B. H. Chung and J.-D. Kim, *J. Mater. Chem. B*, 2013, **1**, 3035.
4. Y. Lu, P. S. Low, *Adv. Drug Deliv. Rev.*, 2012, **64**, 342.
5. S. D. Raghvendra, K. T. Rakesh and K. J. Narendra, *Curr. Drug Deliv.*, 2013, **10**, 477.
6. A. Okamatsu, K. Motoyama, R. Onodra, T. Higashi, T. Koshigoe, Y. Shimada, K. Hattori, T. Takeuchi and H. Arima, *Bioconjugate Chem.*, 2013, **24**, 724.
7. L. Niu, L. Meng and Q. Lu, *Macromol. Biosci.*, 2013, **13**, 735.
8. R. W. Naumann, R. L. Coleman, R. A. Burger, E. A. Sausville, E. Kutarska, S. A. Ghamande, N. Y. Gabrail, S. E. Depasquale, E. Nowara, L. Gilbert, R. H. Gersh, M. G. Teneriello, W. A. Harb, P. A. Konstantinopoulos, R. T. Penson, J. T. Symanowski, C. D. Lovejoy, C. P. Leamon, D. E. Morgenstern and R. A. Messmann, *J. Clin. Oncol.*, 2013, **31**, 4400; E. Sausville, P. LoRusso, M. Quinn, K. Forman, C. Leamon, D. Morganstern, S. Bever and R. Messmann, *J. Clin. Oncol.*, 2007, **25**, 2577.
9. R. E. Fisher, B. A. Siegel, S. L. Edell, N. M. Oyesiku, D. E. Morgenstern, R. A. Messmann, R. J. Amato, *J. Nucl. Med.* 2008, **49**, 899.
10. Y. S. Yi, W. Ayala-López, S. A. Kularatne and P. S. Low, *Mol. Pharm.*, 2009, **6**, 1228.
11. Y. Y. J. Gent, K. Weijers, C. F. M. Molthoff, A. D. Windhorst, M. C. Huisman, D. E. C. Smith, S. A. Kularatne, G. Jansen, P. S. Low, A. A. Lammertsma and C. J. van der Laken, *Arthritis Res. Ther.*, 2013, **15**:R37, 1 and references therein.
12. P. S. Low, W. He, E. Vlashi, J. X. Chen and M. Kennedy, *Microsc. Microanal.*, 2007, **13**, 346.
13. S. Hong, P. R. Leroueil, I. J. Majoros, B. G. Orr, J. R. Baker and M. M. B. Holl, *Chem. Biol.*, 2007, **14**, 107.
14. M. Barz, F. Canal, K. Koynov, R. Zentel and J. M. Vicent, *Biomacromolecules*, 2010, **11**, 2274 and references therein.
15. J. E. Silpe, M. Sumit, T. P. Thomas, B. Huang, A. Kotlyar, M. A. van Dongen, M. M. Banaszak Holl, B. G. Orr and S. K. Choi, *ACS Chem. Biol.*, 2013, **8**, 2063.
16. S. B. Nimsea and T. Kim, *Chem. Soc. Rev.*, 2013, **42**, 366.
17. G. M. L. Consoli, G. Granata, E. Galante, I. Di Silvestro, L. Salafia and C. Geraci, *Tetrahedron*, 2007, **63**, 10758.
18. C. Geraci, G. M. L. Consoli, E. Galante, E. Bousquet, M. Pappalardo and A. Spadaro, *Bioconjugate Chem.*, 2008, **19**, 751.
19. C. Geraci, G. M. L. Consoli, G. Granata, E. Galante, M. Pappalardo and A. Spadaro, *Bioconjugate Chem.*, 2013, **24**, 1710.
20. G. M. L. Consoli, F. Cunsolo, C. Geraci and V. Sgarlata, *Org. Lett.*, 2004, **6**, 4163.
21. R. Lalor, H. Baillie-Johnson, C. Redshaw, S. E. Matthews and A. Mueller, *J. Am. Chem. Soc.*, 2008, **130**, 2892; Z. Qin, D.-S. Guo, X.-N. Gao and Y. Liu, *Soft Matter*, 2014, **10**, 2253.
22. G. M. L. Consoli, G. Granata and C. Geraci, *Org. Biomol. Chem.*, 2011, **9**, 6491.

23. G. Granata, G. M. L. Consoli, S. Sciuto and C. Geraci, *Tetrahedron Lett*., 2010, **51**, 6139.
24. N. W. McGill and S. J. Williams, *J. Org. Chem.*, 2009, **74**, 9388.
25. Y. Lin, R. Weissleder and C.-H. Tung, *Bioconjugate Chem*., 2002, **13**, 605.
26. A. Mueller, R. Lalor, C. Moyano Cardaba and S. E. Matthews, *Cytrometry Part A*., 2011, **79A**, 126.
27. W. H. Kim, J. Lee, D.-W. Jung and D. R. Williams, *Sensors*, 2012, **12**, 5005.
28. C. D. Hein, X.-M. Liu and D. Wang, *Pharm. Res*., 2008, **25**, 2216.
29. J. Luo, M. D. Smith, D. A. Lantrip, S. Wang and P. L. Fuchs, *J. Am. Chem. Soc*., 1997, **119**, 10004.
30. S. Wang, J. Luo, D. A. Lantrip, D. J. Waters, C. J. Mathias, M. A. Green, P. L. Fuchs and P. S. Low, *Bioconjugate Chem*., 1997, **8**, 673.
31. C. Chen, J. Ke, E. X. Zhou, W. Yi, J. Brunzelle, J. Li, E.-L. Yong, E. H. Xu and K. Melcher, *Nature*, 2013, **500**, 486.
32. C. P. Leamon and P. S. Low, *Proc. Natl. Acad. Sci. U.S.A*., 1991, **88**, 5572.
33. L. M. Bareford and P. W. Swaan, *Adv. Drug Delivery Rev*., 2007, **59**, 748.
34. P. K. Eggers, T. Becker, M. K. Melvin, R. A. Boulos, E. James, N. Morellini, A. R. Harvey, S. A. Dunlop, M. Fitzgerald, K. A. Stubbs and C. L. Raston, *RSC Advances*, 2012, **2**, 6250; V. Bagnacani, V. Franceschini, M. Bassi, M. Lomazzi, Donofrio, F. Sansone, A. Casnati and R. Ungaro, *Nature Commun.*, 2013, **4**, 1.
35. C. Redshaw, M. R. J. Elsegood, J. A. Wright, H. Baillie-Johnson, T. Yamato, S. De Giovanni and A. Muller, *Chem. Commun*., 2012, **48**, 1129.
36. K. Kawano and Y. Maitani, *J. Drug Deliv*., 2011, ID 160967.
37. E. Vlashi, L. E. Kelderhouse, J. E. Sturgis and P. S. Low, *ACSNano*, 2013, **7**, 8573.
38. K. Zang, R. Rossin, A. Hagooly, Z. Chen, M. J. Welch and K. L. Wooley, *J. Polym. Sci. A Polym. Chem*., 2008, **46**, 7578.
39. A. Galbiati, C. Tabolacci, B. Morozzo Della Rocca, P. Mattioli, S. Beninati, G. Paradossi and A. Desideri, *Bioconjugate Chem*., 2011, **22**, 1066.
40. A. Gabizon, A. T. Horowitz, D. Goren, D. Tzemach, F. Mandelbaum-Shavit, M. M. Qazen and S. Zalipsky, *Bioconjugate Chem*., 1999, **10**, 289.
41. B. A. Kamen and A. Capdevila, *Proc. Natl. Acad. Sci. U.S.A*., 1986, **83**, 5983.
42. J. Huotari and A. Helenius, *EMBO J*., 2011, **30**, 3481.
43. P. Saftig and J. Klumperman, *Nature Rev. Mol. Cell Biol*., 2009, **10**, 623.
44. C. Dua, D. Denga, L. Shana, W. Shunan, J. Caoa, J. Tiana, S. Achilefub and Y. Gu, *Biomaterials* 2013, **34**, 3087.
45. B. Kang, D.-C. Yu, S.-Q. Chang, D. Chen, Y.-D. Dai and Y. Ding, *Nanotechnology*, 2008, **19**, 375103.
46. H. Yang, C. Lou, M. Xu, C. Wu, H. Miyoshi and Y. Liu, *Int. J. Nanomedicine*, 2011, **6**, 2023.
47. M. Baldassarre, A. Pompeo, G. Beznoussenko, C. Castaldi, S. Cortellino, M. A. McNiven, A. Luini and R. Buccione, *Mol. Biol. Cell*, 2003, **14**, 1074.
48. T. Pulvirenti, M. Giannotta, M. Capestrano, A. Capitani, R. S. Pisanu, E. Polishchuk, G. V. San Pietro, A. A. Beznoussenko, G. Mironov, G. Turacchio, V. W. Hsu, M. Sallese and A. Luini, *Nat. Cell Biol*., 2008, **10**, 912.